Feasibility Study of Real Time Path Tracing

Or: How Much Noise Is Too Much?

A thesis submitted for the degree of

Bachelor of Science
in
Computer Science

by

Sven-Hendrik Haase
Matriculation number: 6341873

Department of Computer Science
University of Hamburg
Germany

Primary Supervisor: Prof. Dr. rer. nat. Leonie Dreschler-Fischer
Secondary Supervisor: Prof. Dr. Thomas Ludwig

Abstract

This study aims to investigate the viability of a physically based technique called *path tracing* in lieu of or in corporation with classical techniques in interactive media such as video games and visual effects tools.

Real time path tracing has been prohibitively expensive in regards to computational complexity. However, modern GPUs and even CPUs have finally gotten fast enough for real time path tracing to become a viable alternative to traditional real time approaches to rendering. Based on that assumption, this thesis presents the idea, algorithm and complexity behind path tracing in the first part, and extrapolates feasibility and suitability of real time path tracing on consumer hardware according to the current state of technology and trends in the second part.

As part of the research, the author has implemented a path tracing 3D engine in modern C++ in order to empirically test the assumptions made in this thesis. The data suggests that path tracing may be a viable rendering technique for upper level commodity hardware in approximately four years.

Acknowledgments

I would like to express my sincere gratitude to the teachers throughout school and university for the knowledge they've passed on. I thank my friends for the laughs, mistakes and triumphs we shared with one another.

Furthermore, none of this would have been possible without the incredible efforts and love of my parents who have supported me throughout the years and enabled me to live a carefree life until I was ready to fend for myself.

Lastly, but certainly not least, I would like to declare my gratefulness to Alisa, whose endless love has given my life a new meaning.

We all make choices in life, but in the end, our choices make us.

Andrew Ryan

Contents

Acronyms

AABB axis-aligned bounding box

AO ambient occlusion

BRDF bidirectional reflection distribution function

BVH bounding volume hierarchy

BSP binary space partitioning

CPU central processing unit

CSG constructive solid geometry

FPS frames per second

GI global illumination

GPU graphics processing unit

PSNR Peak signal-to-noise ratio

HDR high dynamic range

GFLOPS billions of floating point operations per second

MLT Metropolis light transport

PBR physically based rendering

RT real time

RGB red-green-blue

SIMD single instruction multiple data

SPP samples per pixel

SSAO screen-space ambient occlusion

1 Introduction

As part of the quest for ever-improving game graphics, researchers, graphics hardware developers and video game developers alike have been coming up with more and more convoluted and technically challenging ways of improving the graphics in interactive media such as games and visualizations in order to give users a deeper sense of immersion or to provide special effects artists with faster feedback.

While rendering techniques are currently shifting from the traditional fixed pipeline approach towards the new, fully programmable approach that lets developers implement deferred renderers that can more closely mimic reality by using multiple combined shading and lighting algorithms and rendering the scene multiple times for different buffers, the fundamental concept of rasterization-based rendering has largely remained the same.

The real world photon-collecting approach that actual cameras use has so far not been adopted for interactive media by the industry in any capacity because the computational cost has historically been prohibitively expensive. It is, however, used extensively (and has been in use for decades) for offline, non-interactive rendering of computer-generated movies and visualizations of scientific simulations.

This study assumes that the next logical step for the industry will be to adopt this method for real time media as well. For the purpose of this thesis, a renderer is considered *real time* when it manages to render a frame within $16.67ms$ since that equals 60 frames per second (FPS) which is the current de facto standard refresh rate for most available computer screens. Conversely, a renderer is called *offline* when it is not designed for interactive rendering which usually means that it will renderer an image or a batch of images over the course of a few days. The differences of real time and offline path tracing renderers will be explained in the next chapter.

The focus of this research is, first and foremost, interactivity. Therefore, whenever a trade-off between interactivity and image quality is considered, we will always prefer rendering speed if the target of 60 FPS would otherwise not be reached anymore.

1.1 Motivation

Real time path tracing (and physically based rendering in general) offers many benefits over traditional real time rendering methods such as better visuals and simpler implementation but also allows for completely new types of graphics such as realistic caustics [1] and even light dispersion [2] (using a prism, for instance) since path tracers might simulate wavelengths instead of plain red-green-blue (RGB) colors. Modern video games tend to rely on a growing number of tricks to keep them visually appealing as the consumer grows more demanding. They're called *tricks* in this study because they merely trick the beholder into seeing something that appears to be physically accurate when it is, in fact, not the result of a physically based calculation and as such this study aims to keep tricks and emergent phenomena separated by language. Some notable tricks include screen-space ambient occlusion (SSAO) [3], motion blur [4], lens flares [5], chromatic aberration [6], depth of field [7] and light mapping [8].

1.2 Leading Questions and Goals

The primary research objective of this thesis is finding out when real time path tracing will be a viable alternative to rasterization on commodity desktop hardware. This question is explored by looking at theoretical indicators (such as peak floating point performance and performance projections) and practical indicators (by implementing a real time path tracer and benchmarking it).

2 Real Time Path Tracing Explained

This chapter will explain the concepts, mathematics, physics and algorithms behind path tracing, how real time path tracing differs from offline path tracing and the trade-offs made to achieve acceptable performance. It will also explain how path tracing differs from rasterization and common global illumination (GI) techniques.

2.1 Physically Based Approach

In our physical world, we see pictures because our eyes collect photons emitted by light sources which then bounce around various surfaces until they eventually hit our eyes' photoreceptor cells. On every bounce, a bit of light is absorbed which is why light loses intensity when it bounces. Some surfaces absorb a particular band of wavelengths of the light when it bounces which we perceive as a change in the light's color. Cameras work exactly like this as far as collection of photons is concerned.

This physical approach would be extremely wasteful and computationally complex to simulate, however, since most photons never reach an observer. Consider, for instance, that only an extremely small percentage of all the photons sent by the Sun actually reach Earth and an even smaller percentage of those are ever observed (although photons don't have to be observed to have a physical effect, of course). Since we only care for photons that are relevant to the image that we are trying to render, it makes more sense to use *backwards ray tracing* in which rays (which simulate streams of photons) are shot from the observer into the scene for every sensor. It is called *backwards* because the rays are traced in the reverse direction compared to their physical counterparts.

This is efficient since we usually only care about a single observer (the scene camera) for which we will trace every single ray that it can possibly perceive. In computer graphics terms, we will trace a ray for every pixel of the camera (and for now we will assume that the viewport is exactly the same resolution as the camera for simplicity's sake). For every ray, we check for intersections with geometry and then either bounce a few more times or shoot directly towards a light. We might do this multiple times per

pixel and integrate all resulting values to improve image quality. This type of sampling is called *Monte Carlo integration*. The more iterations we spend on sampling, the better the quality of our image becomes. This is called *converging*.

There are a many approaches that improve this completely random approach to sampling. While the most straightforward approach is given by uniform sampling, other methods such as stratified sampling [9] and importance sampling [9] will usually provide a clear advantage in terms of time to convergence. Other, more complicated approaches are bidirectional path tracing [10] in combination with Multiple Importance Sampling [9] and the Metropolis light transport (MLT) [11] which shoot rays from both the light and the camera and then connect all the intersection points in order to form a light path.

2.2 Theoretical Basis

2.2.1 The Rendering Equation

The fundamental problem solved by path tracing is the *rendering equation* originally described by James Kajiya [12].

$$L_\mathrm{o}(\mathbf{x}, \omega_\mathrm{o}, \lambda, t) = L_\mathrm{e}(\mathbf{x}, \omega_\mathrm{o}, \lambda, t) + \int_\Omega f_\mathrm{r}(\mathbf{x}, \omega_\mathrm{i}, \omega_\mathrm{o}, \lambda, t)\, L_\mathrm{i}(\mathbf{x}, \omega_\mathrm{i}, \lambda, t)\, (\omega_\mathrm{i} \cdot \mathbf{n})\, \mathrm{d}\,\omega_\mathrm{i}$$

For our purposes, this can be simplified by removing the time and wavelength components which we will not make use of:

$$L_\mathrm{o}(\mathbf{x}, \omega_\mathrm{o}) = L_\mathrm{e}(\mathbf{x}, \omega_\mathrm{o}) + \int_\Omega f_\mathrm{r}(\mathbf{x}, \omega_\mathrm{i}, \omega_\mathrm{o})\, L_\mathrm{i}(\mathbf{x}, \omega_\mathrm{i})\, (\omega_\mathrm{i} \cdot \mathbf{n})\, \mathrm{d}\,\omega_\mathrm{i}$$

This equation can be broken down into its individual parts to make it easier to explain and understand:

$$L_\mathrm{o}(\mathbf{x}, \omega_\mathrm{o}) = L_\mathrm{e}(\mathbf{x}, \omega_\mathrm{o}) + \int_\Omega f_\mathrm{r}(\mathbf{x}, \omega_\mathrm{i}, \omega_\mathrm{o})\, L_\mathrm{i}(\mathbf{x}, \omega_\mathrm{i})\, (\omega_\mathrm{i} \cdot \mathbf{n})\, \mathrm{d}\,\omega_\mathrm{i}$$

$L_\mathrm{o}(\mathbf{x}, \omega_\mathrm{o})$ is the **outgoing light** with $\mathbf{x}$ being a point on a surface from which the light is reflected from into direction ω_o.

$L_\mathrm{e}(\mathbf{x}, \omega_\mathrm{o})$ is the **emitted light** from point $\mathbf{x}$. Usually surfaces don't emit light themselves unless they are area lights.

$\int_\Omega \ldots \mathrm{d}\,\omega_\mathrm{i}$ is the integral over Ω which is the hemisphere at $\mathbf{x}$ (and thusly centered

around $\mathbf{n}$). All possible values for ω_i are therefore contained in Ω.

$f_\mathrm{r}(\mathbf{x}, \omega_\mathrm{i}, \omega_\mathrm{o})$ is the **bidirectional reflection distribution function (BRDF)** which determines how much light is reflected from ω_i to ω_o at $\mathbf{x}$.

$L_\mathrm{i}(\mathbf{x}, \omega_\mathrm{i})$ is the **incoming light** at $\mathbf{x}$ from ω_o. It is not necessarily *direct light*. The rendering equation also considers *indirect light* which is light that has already been reflected.

$(\omega_\mathrm{i} \cdot \mathbf{n})$ is the **normal attenuation** at $\mathbf{x}$. The incoming light ω_i is weakened depending on the cosine of the angle between ω_i and the surface normal $\mathbf{n}$.
Path tracing offers a numerical solution to the integral found in this equation. For every pixel, every bounce and every sample of the camera, the rendering equation is solved. Considering this, it becomes apparent why this is an expensive algorithm to run. For practical reasons, not every possible value for Ω is sampled since this would take a vast amount of time to calculate at physical photon density. Instead, only a few possible values for Ω are calculated each bounce. Depending on the exact algorithm used, usually only a low number of samples (approximately 20) is required for the image to converge to an acceptable level of quality.

2.2.2 Algorithm

The general naive algorithm for path tracing in Python-like pseudocode for diffuse and emissive materials can be written as follows:

```
max_depth = 5
scene = [triangle_1, ..., triangle_n] # Many triangles defined here

def trace_ray(ray, depth):
    if depth >= max_depth:
        # Return black since we haven't hit anything but we're
        # at our limit for bounces
        return RGB(0, 0, 0)

    intersection = None
    for triangle in scene:
        intersection = check_intersection(ray, triangle)
        if intersection:
            # Break at first intersection
```

```
            break

    if not intersection:
        # If we haven't hit anything, we can't bounce again so
        # we return black
        return RGB(0, 0, 0)

    material = intersection.material;
    emittance = material.emittance

    # shoot a ray into random direction and recurse
    next_ray = Ray()
    next_ray.origin = intersection.position
    next_ray.direction = random_vector_on_hemisphere(intersection.normal)

    reflectance_theta = dot(next_ray.direction, intersection.normal)
    brdf = 2 * material.reflectance * reflectance_theta
    reflected = trace_ray(next_ray, depth + 1)

    return emittance + (brdf * reflecte)

for sample in range(samples):
    for pixel in pixels:
        trace_path(ray_from_pixel(pixel), 0)
```

Listing 1: Naive path tracing algorithm

The algorithmic complexity of this algorithm is not immediately obvious because of its pseudocode character and a few methods whose implementations are not provided. It is known, however, that the output image Out will be a 2D matrix with dimensions given by width w and height h. Additionally, for every pixel, multiple samples s are required in order for the algorithm to converge to an image of acceptable quality. Every ray has a certain maximum depth d. The scene has n triangles. We will assume the functions `check_intersection`, `random_vector_on_hemisphere` and `dot` to run in constant time.

If we consider s and d to be constant, the remaining variables will be the total number of pixels ($w*h$) and the total number of triangles (n). We can then see that the algorithm in listing 1 runs in $O(n^2)$ since we have to check every triangle for every ray.

Knowing that, it is possible to determine the total worst number of scene intersection tests required per image. In the worst case, no ray exits before reaching its maximum depth. The resulting formula is:

$$w \times h \times s \times d \times n \tag{2.1}$$

Using formula 2.1, the maximum number of scene intersection tests can be calculated by assigning some sensible real world values to all symbols:

Number of triangles n	Intersection in $O(n)$	Intersection in $O(\log(n))$
10	3,110,400,000	622,080,000
100	31,104,000,000	1,555,200,000
1,000	311,040,000,000	2,177,280,000
10,000	3,110,400,000,000	2,799,360,000
100,000	31,104,000,000,000	3,732,480,000
1,000,000	311,040,000,000,000	4,354,560,000

Table 2.1: Worst case number of total scene intersection tests using formula 2.1 with $w = 1920, h = 1080, s = 30, d = 5$

As table 2.1 shows, the number of scene intersection tests quickly escalates as we add more triangles if we use an intersection test that checks against every triangle (making it run in $O(n)$). The table shows much more manageable numbers assuming the scene intersection could be done in $\log(n)$. If the latter were the case, the whole algorithm would run in $O(n \log(n))$ instead of $O(n^2)$ as in the naive algorithm 1.

2.2.3 Acceleration Data Structures

The data structure used for the underlying scene is the principal factor for the performance of the path tracing algorithm. The most commonly used naive data structure for path tracing is a simple list of shapes. Upon scene lookup, a ray is tested for intersection with every shape. The complexity in this case is $O(n)$ where n is the number of shapes which is comparable to rasterization but a lot worse than it could be with a proper acceleration data structure.

Assuming a flat list of shapes as the current data structure, the next logical step to improve scene look up time is to add axis-aligned bounding boxes (AABBs) around clusters of smaller shapes. For instance, an AABB might surround an icosahedron shape that is made up of hundreds of triangles. This way, the triangles inside the AABB are only tested for ray intersections if the ray intersects the AABB that surrounds the shape. The complexity is now $O(m \cdot n)$ where m is the number of shapes (which is equal to the number of AABBs) and n is the number of triangles. While this is a worse complexity class compared to before, the number of comparisons is a lot lower in practice because m is always smaller than n (usually by magnitudes) and n is only relevant if a shape was hit.

The next iteration on top of simple AABBs is provided by tree-based acceleration data structures. The most commonly used ones are the bounding volume hierarchy (BVH) and the kd-tree. By using these data structures, scene lookup performance per ray could be drastically improved to $O(\log n)$ at the cost of a tree rebuild once per frame. This is usually a good trade-off since a scene is looked up millions of times per frame but the tree only has to be rebuilt once. While there are multiple ways to build a BVH, most of them have a complexity close to $O(n(\log n))$. A kd-tree is usually built in $O(n(\log n))$ as well.

2.3 Properties of Path Tracing

This section summarises the general properties of path tracing.

Computational Cost Even though path tracing has a high initial cost as shown in section 2.2.2, the lookup time for ray collisions is in $O(\log n)$ which means that as scenes increase in complexity, the time spent on doing the lookups is fairly small. The initial cost of path tracing heavily depends upon screen resolution and desired quality. Due to the high initial cost, path tracing is generally considered slow and it made real time path tracing infeasible up until recent years.

Dynamic Scenes Path tracing is well suited for dynamic scenes since it doesn't depend on pre-computations. This makes it viable for use in interactive applications. The scene data structure must allow for dynamic scenes in this case, though.

Global Illumination Path tracing is one of many ways of simulating global illumination (GI). Commonly GI refers to a class of algorithms that simulate direct as well as indirect lighting in a scene. This implies that every object's illumination affects every other object and that the renderer doesn't make a distinction between

reflected light and light sources.

Problems Due to the unbiased and random way rays are reflected from surfaces, it takes a long time for classic path tracing to produce sharp caustics as rays tend to very rarely hit objects with caustic properties. This makes it especially difficult for real time path tracing to produce sharp caustics. This can be alleviated by using bidirectional path tracing [10] or by using an additional photon map as well as Multiple Importance Sampling [9].

Another problem is that subsurface scattering and participating media such as smoke can't be calculated by classic Monte Carlo path tracers. This can be addressed by using *volumetric path tracing*. [13] [14]

Since path tracers do not simulate light wavelengths, natural phenomena caused by chromatic aberration, fluorescence and iridescence can not be realistically simulated. A fairly new improvement to path tracing called *spectral path tracing* with realistic lenses can produce physically accurate images in those cases. [15] [16] [17] [18]

2.3.1 Comparison to Traditional Ray Tracing

Ray tracing is the fundamental algorithm behind path tracing. The only difference is that when a ray hits an object, it doesn't keep bouncing but instead fires off one ray to every light source directly. This subtle difference means that ray tracing can only calculate direct lighting as opposed to GI. It also makes ray tracing much less expensive from a stand point of computation. Images produced with this method lack realism and depth. Many physical effects can't be calculated this way.

2.3.2 Comparison to Rasterization

Rasterization is widely implemented in the industry and most interactive 3D applications use it to render their scene. Its fundamental algorithm has a complexity of $O(n)$ and is therefore theoretically slower than path tracing. However, a wide array of algorithmic improvements such as back-face culling exist and additionally its initial cost is very low.

Unlike path tracing, it does not automatically simulate a wide range range of physical phenomena. Physical effects such as shadows, global illumination and caustics have to be calculated separately in other algorithms and then be composited on top of the rasterized scene. This makes rasterization complicated in cases where many physically

based effects are desired.

2.3.3 Comparison to Other Global Illumination Algorithms

This section compares some of the more popular GI algorithms beside ray tracing and path tracing. In general, GI is considered to be a group of algorithms that calculate direct light as well as indirect light for computer graphics scenes. However, not all algorithms that fulfill this purpose are in fact physically accurate. We will therefore take a look at how some of these algorithms compare to path tracing.

The algorithms that are compared to path tracing in this section are: *photon mapping*, *radiosity* and *ambient occlusion*. These were chosen due to their widespread use and their varied approaches. Other GI algorithms include: Lightcuts (and its variants), Point Based Global Illumination and Spherical harmonic lighting.

To note: This thesis considers path tracing at the current state of research which means that path tracing, bidirectional path tracing and the MLT are shortened to just *path tracing* and will therefore not be individually compared.

Photon Mapping

Photon mapping is a two-step process that was developed in 1996 by Henrik Wann Jensen [19] as an approximate way to simulate charged particles (*photons*) traversing the scene.

In the first step, every photon carries a *charge* and is traced through the scene. On every collision with scene geometry, it is stored to the *photon map* at that location. Afterwards, the photon is either reflected, refracted, scattered or absorbed depending on the material and loses a bit of its charge. The photon map serves as a cache for the second step in which a ray tracing-like process is used to calculate the radiance of the resulting image.

Compared to path tracing, photon mapping has a few advantages and a few disadvantages. In particular, photon mapping can simulate subsurface scattering and volume caustics which path tracing can't accurately calculate. On the other hand, photon mapping is unsuitable for real time applications with dynamic scenes since the photon map can only be used as long as the scene geometry or light position doesn't change. In the case the scene geometry changes, the cache is invalidated and a new photon map has to be calculated which is a slow process.

Radiosity

Made originally for simulating heat transfer in 1984 by Goral et al.[20], radiosity is one of the oldest algorithms for calculating GI. It outputs a light value for every patch (a smaller part of a surface) on a cache or map. It is a physically accurate way of simulating light transfer but cannot simulate volume scattering, fog, caustics, transparent objects or mirrors. These limitations make it unsuitable to use in complex modern scenes. Additionally, the cache is invalidated whenever the scene changes and therefore it is also usually not usable for dynamic scenes.

Ambient Occlusion

The idea for ambient occlusion (AO) was first presented by Gavin Miller in 1994 [21]. It is meant as an algorithm to calculate realistic occlusion of every point in a scene and cannot generate an accurate image on its own. It is usually used with a classic rasterization renderer whose output image is multiplied with the result of the AO and its resulting image is multiplied. The output of this algorithm is sometimes called the *ambient occlusion map* which serves as a cache. As such, rendering is extremely fast once the cache has been calculated. However, this cache is invalidated once the scene changes and is the algorithm is therefore unsuitable for dynamic scenes.

For real time applications, a variant of AO called screen-space ambient occlusion (SSAO) is usually used. While SSAO is inaccurate from a physical point of view, it results in some very fast and acceptable approximations that are suitable for real time applications.

2.4 History of Path Tracing

As with so many things in computer science and science in general, the modern idea of physically based rendering using path tracing builds upon many important past discoveries and algorithms such as ray tracing and ray casting. Arthur Appel is generally credited as being the father of *ray casting* as he was the first to describe the algorithm in a 1968 paper [22].

Ray casting is an important idea needed for *ray tracing* which was first published in a paper in 1980 by Turner Whitted [23].

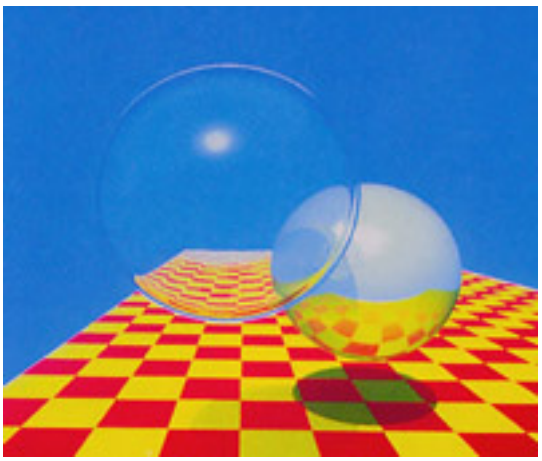

Figure 2.1: Turner Whitted's original 1980 [23] image showing off the usage of ray tracing for reflection, refraction and shadows.

Building upon ray tracing, an improved algorithm was published in 1986 by James T. Kajiya which used ray tracing combined with a Monte Carlo algorithm in order to create a new algorithm that was called *Monte Carlo ray tracing* [12]. Nowadays, Monte Carlo ray tracing is better known as *path tracing*.

It took another decade for path tracing to become the physically based rendering approach that it is known for today. In 1996, Eric Lafortune improved the algorithm by suggesting the usage of bidirectional path tracing [10] and finally the MLT was suggested in 1997 by Eric Veach and Leonidas J. Guibas [11] to improve performance in complex scenes.

This was the last notable improvement to the algorithm, though many micro optimizations have since been published. All of these achievements and improvements are generally collapsed into the term *path tracing* since they do not diverge from the general algorithm but instead improve upon it.

It took longer still for the industry to become interested in path tracing. The early interest in ray tracing was of mostly academical and recreational nature. One of the most notable creations of the early days of ray tracing is *The Juggler* created and published by Eric Graham in 1986 [24] on an Amiga 1000. It was a pre-rendered animation using ray tracing. Eric Graham stated that it took the Amiga 1 hour to render each frame [24].

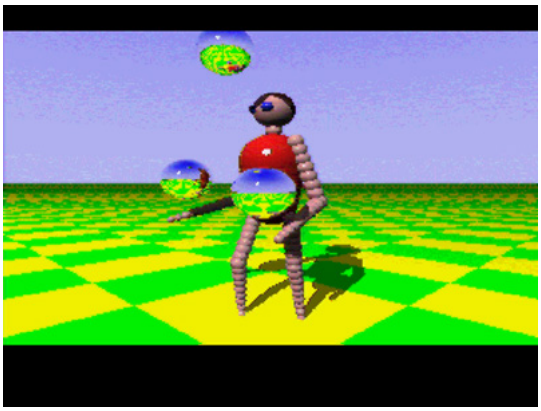

(a) Eric Graham's Juggler

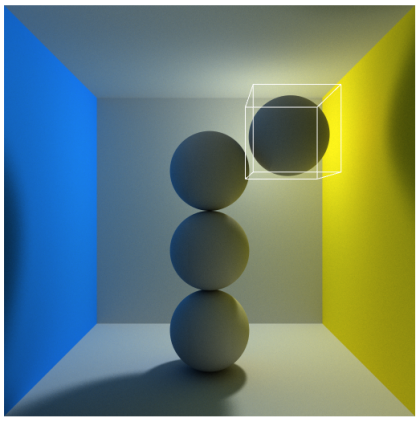

(b) WebGL Path Tracer by Evan Wallace

While the animation seems very primitive compared to the animations of today, it was exceptional at the time. Ernie Wright's statement about his creation provides some contemporary context:

> Turner Whitted's paper (1980) is widely regarded as the first modern description of ray tracing methods in computer graphics. This paper's famous image of balls floating above a checkerboard floor took 74 minutes to render on a DEC VAX 11/780 mainframe, a $400,000 computer. The Juggler would appear a mere six years later, created and displayed on a $2000 Amiga. ([24])

The first feature-length computer-animated film, *Toy Story*, released in 1995 [25], is sometimes miscredited as being the first film using a ray tracing-like algorithm. However, it actually used traditional scanline rendering. The first feature-length film using ray tracing, *Cars*, was released much later, in 2006 [26] [27] and started a wave of interest in the movie industry.

The first example of *real time* path tracing was likely produced by the demo scene [28] which was quick to adopt it [29] for the purpose of producing complex graphics rendered and generated on the fly. One notable example of this is the WebGL Path Tracing by Evan Wallace made in 2010 [30] which runs in most modern web browsers, making path tracing very accessible.

Another example is the demo *5 faces* by Fairlight from 2013 [31] which uses a real time ray tracer running on the GPU to render a complex scene at 30 FPS.

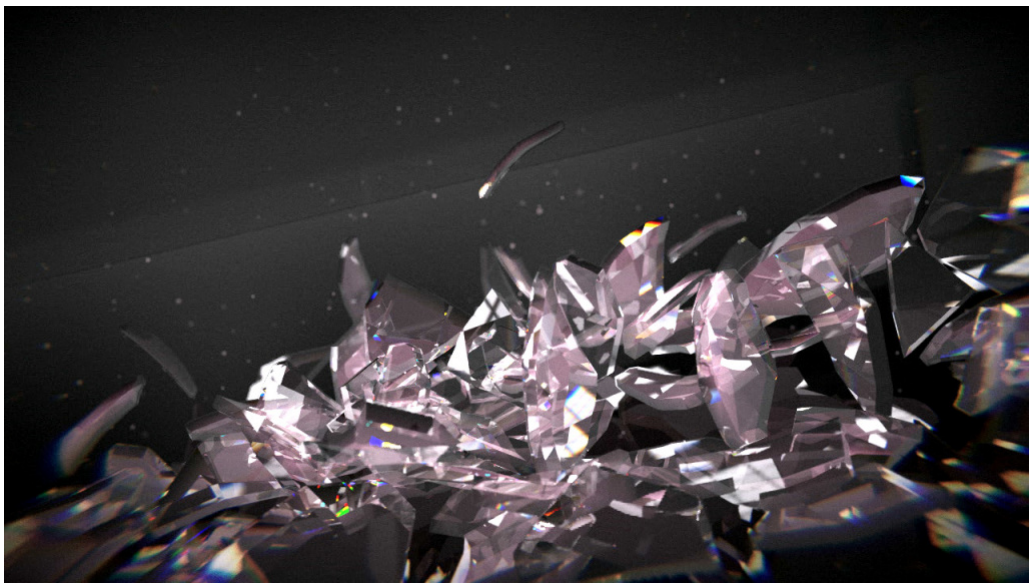

Figure 2.2: 5 faces by Fairlight

In the past, some critics have offered critical insights about why it might not be a viable alternative to rasterization on consumer hardware in the short term [32] [33]. Even John Carmack of id Software was sceptical of real time ray tracing in games in 2012 in a comment on Ars Technica [34].

2.5 Current State of Technology

Recent interest in real time path tracing is at peak levels. The most notable example of this is Jacco Bikker's and Jeroen van Schijndel's *Brigade Renderer* [35] [36]. This renderer is aimed at game developers and is meant to run on commodity hardware in real time. Its company, OTOY, is also developing a cloud-based rendering solution called Octane Render [37] for animation professionals.

Microsoft's DirectX 12 [38] is receiving *Hybrid Ray-Traced Shadows*, a technology that combines real time ray tracing with rasterization to create fast high quality shadows.

A video game using actual real time path tracing and physics called *Sfera* was created by David Bucciarelli [39] in 2011. It uses OpenCL for calculating the paths and OpenGL to render them to the screen.

It's important to keep in mind that while the real time graphics industry has mostly been driven by video games, the most important hardware currently exist in game consoles which generally evolve at a much slower pace than desktop computers in terms of hardware power and their graphics hardware especially is usually non-upgradeable. This means that it wouldn't be economically viable to develop a real time path tracing renderer that only ran on current generation desktop computers because most consumers would not be able to benefit from the technology.

3 Research

The entirety of the practical research in this thesis was done with a Monte Carlo path tracer called *trac0r* [40]. An effort was made to find an existing open source implementation of a path tracer focused on real time applications but none seem to exist as of this writing. The most likely cause for that is the enormous hardware cost currently still associated with doing real time path tracing.

3.1 Implementation

Alongside this thesis, a Monte Carlo path tracer called trac0r [40] was implemented in C++14. It uses a library called glm [41] for linear algebra and most other mathematical operations. Since trac0r itself is only a library, a graphical application making use of it was implemented to showcase its results. This application is called *trac0r_viewer* and uses SDL2 [42] for input and output. trac0r_viewer allows for interactive scene navigation, visual debugging and automatic benchmarking.

A conscious decision was made to only implement triangles for geometric primitives due to two reasons. Firstly, since every other geometric shape can be expressed easily using an amount of triangles, it seems unnecessary to add additional complexity (although using triangles to approximate other shapes will be less efficient from a performance perspective). Secondly, real world applications very rarely make use of perfect mathematical shapes such as spheres, boxes and tori when rendering. Most modern mesh modeling approximates these shapes using triangles. Since this renderer is supposed to be used for real world application such as games and interactive visualizations, it didn't seem necessary to implement anything in addition to what mesh modeling tools will export.

Additionally to triangles, AABBs were implemented with the aim to speed up rendering. While trac0r does not implement any advanced acceleration structures (such as BVHs or kd-trees), it uses AABBs to dramatically decrease the number of triangle intersection tests. Every ray first tests for intersections with every AABB in the scene

and upon a hit tests every triangle enclosed by the AABB. The fast Möller–Trumbore intersection algorithm [43] is used for triangle intersection tests.

The program does not currently support importing of externally defined scenes or meshes. Scenes are defined in-code. Methods for generating planes, boxes and icosahedra out of triangles are provided. A properly sized AABB is built around every shape.

It uses classic reverse path tracing and can optionally make use of OpenCL or OpenMP in order to speed up computation.

3.1.1 Design Overview

When deciding to implement a path tracer, one first has to assemble a list of requirements and components that go into creating it. Not all path tracers are built the same.

The list of requirements for trac0r before it was implemented ordered by descending priority is provided below:

1. **Speed**. In a real time path tracer, rendering speed is of utmost importance as one needs to target interactive frame rates at acceptable image quality. The trade-off here is that the image is allowed to be grainy as long as it can be shown to the user very quickly.
2. **Ease of implementation**. Since the nature and scope of this thesis does not allow for implementing the most advanced algorithms, the only constraint for the implementation is for it to be good enough for benchmarking.
3. **Interactivity**. The path tracer should show off basic interactivity. It should be noted, however, that it will probably not reach the requirements for *real time* as lined out in chapter 1 due to hardware constraints.
4. **Portability**. The software should run on different GPUs as well CPUs with different memory and core configurations respectively with minimal effort. It should therefore be written with this portability in mind to make it easier to adapt.
5. **Maintainability**. The software should be easy to understand, well-documented and easy to debug. Code should be commented where necessary.

These requirements and priorities directed and influenced many decisions and trade-offs made during the implementation.

The components that make up the path tracer follow:

Random number generation Solid and fast function for pseudo random number generation.

Camera A structure that keeps all camera data as well as some functions to do coordinate transformations.

Material system The path tracer should support four materials: Emitter, diffuse, glossy, glass. Each of them should at least provide their BRDF.

AABBs A simple way to represent AABBs.

Triangles The only kind of primitive that materials can be applied unto and in fact the only kind of geometry that is rendered.

Shapes and geometry It should provide a way to generate basic geometric shapes. No mechanism for loading externally defined models is planned.

Scene A way to efficiently save an arbitrary number of shapes. At first this should be implemented as a flat list. If there is enough time, a more efficient method should be considered.

Intersection/Scene lookup Implemented as a ray intersection function for each supported primitive (which in this case means ray-AABB intersection and ray-triangle intersection).

Viewer An interactive viewport that shows off progressive rendering with a sample scene.

These components are implemented in the following files:

File(s)	Description
trac0r/aabb.{cpp,hpp}	`AABB` class implementation.
trac0r/camera.{cpp,hpp}	`Camera` class implementation with many helper methods.
trac0r/flat_structure.{cpp,hpp}	Simple flat data structure implementation for scene geometry. Also contains the intersection logic for all contained geometry.
trac0r/intersection_info.hpp	Struct containing all relevant information about a single intersection. This struct is returned by all intersection methods.
trac0r/intersections.hpp	Contains functions for testing primitives for intersections.
trac0r/material.hpp	`Material` struct containing all material state.
trac0r/random.hpp	Implements functions to generate random floating point numbers, integers. Also contains functions for random geometric sampling with uniform and cosine-weighted distributions.
trac0r/ray.hpp	Contains the `Ray` struct which is used by every ray in trac0r.
trac0r/renderer_aux.cl	OpenCL code containing the code for a single trace through the scene. Implements the BRDFs for all materials.
trac0r/renderer_aux.cpp	C++ code containing the code for a single trace through the scene. Implements the BRDFs for all materials.
trac0r/renderer.{cpp,hpp}	Contains code for preparing the OpenCL and C++ renderer.
trac0r/scene.{cpp,hpp}	Simple `Scene` class serving as an abstract interface to the underlying data structure.
trac0r/shape.{cpp,hpp}	Contains a few factory methods for generating different kinds of geometry.
trac0r/timer.hpp	High-resolution timer for profiling purposes.
trac0r/triangle.hpp	A simple struct for expressing a triangle.
trac0r/utils.hpp	Contains various small helper functions for translating OpenCL error codes, packing packing and unpacking colors and displaying text.

Table 3.1: List of files in trac0r

3.1.2 Materials

trac0r implements the following materials:

Emitter Arguably the most important material as it is the one providing the light to a scene. This simulates a black body heated to a certain temperature and as such serves as an area light when applied to geometry. Any ray hitting geometry using the emitter material is terminated. A scene without any geometry using emitter material will be utterly dark.

Diffuse A matte material that scatters light to a random location on the hemisphere around the normal of the intersected geometry.

Glass A material that will choose between reflection and refraction depending on the Fresnel coefficients [44]. It is the only material capable of handling intersections within an object.

Glossy A metal-like material that will reflect a ray towards a cone centered around the direction of the outgoing light ω_o. A roughness parameter determines the opening angle of that cone. A roughness of 0 will result in a perfect mirror while a roughness of 1 will produce a cone with an angle of π.

```
1  struct Material {
2      /**
3      * @brief Used to determine the material type used.
4      * Refer to the table below:
5      *         m_type = 1: Emissive
6      *         m_type = 2: Diffuse
7      *         m_type = 3: Glass
8      *         m_type = 4: Glossy
9      */
10     uint8_t m_type = 1;
11
12     /**
13     * @brief Used as the basic color for most materials.
14     */
15     glm::vec3 m_color = {0.9f, 0.5f, 0.1f};
16
17     /**
18     * @brief Used to determine the ratio between reflection and diffusion
```

```
19      * for some materials. Value must be between 0.0 and 1.0.
20      */
21     float m_roughness = 0.f;
22
23     /**
24      * @brief Index of refraction (IOR) is used to determine how
25      * strongly light is bent inside a glass material.
26      */
27     float m_ior = 1.f;
28
29     /**
30      * @brief Luminous emittance provides the strength of emissive
31      * material. Values can be larger than 1.0.
32      */
33     float m_emittance = 0.f;
34 };
```

Listing 2: Material struct in trac0r. Depending on the `m_type` set, different attributes of this material are used.

3.1.3 Shapes, Triangles and AABBs

In trac0r, shapes are generators for a collection of triangles in a certain configuration. For instance, a `plane` shape generates a list of two triangles that are configured in such a way that they will form a quadratic flat surface with an orientation and scale as provided by the constructor. In addition, shapes also take care of generating a well-fitting AABB.

```
1  class Shape {
2    public:
3      static Shape make_box(glm::vec3 pos, glm::vec3 orientation,
4                            glm::vec3 size, Material material);
5
6      static Shape make_icosphere(glm::vec3 pos, glm::vec3 orientation,
7                                  float radius, size_t iterations,
8                                  Material material);
9
10     static Shape make_plane(glm::vec3 pos, glm::vec3 orientation,
11                             glm::vec2 size, Material material);
```

```
12
13    protected:
14      glm::vec3 m_pos;
15      glm::vec3 m_orientation;
16      glm::vec3 m_scale;
17      AABB m_aabb;
18      std::vector<Triangle> m_triangles;
19  };
```

Listing 3: Shape class in trac0r. The static methods serve as factory functions.

AABBs and triangles are rather simple:

```
1  struct AABB {
2      glm::vec3 m_min;
3      glm::vec3 m_max;
4  };
```

Listing 4: AABB struct in trac0r. Its extents are set by the shape it is part of.

```
1  struct Triangle {
2      glm::vec3 m_v1; // first vertex
3      glm::vec3 m_v2; // second vertex
4      glm::vec3 m_v3; // third vertex
5      Material m_material;
6      glm::vec3 m_normal;
7      glm::vec3 m_centroid;
8      float m_area;
9  };
```

Listing 5: Triangle struct in trac0r. `m_normal`, `m_centroid` and `m_area` are pre-calculated on construction.

3.1.4 Camera and Rays

The camera is configured during the scene setup and sent to the graphics processing unit (GPU) every frame.

```
class Camera {
    glm::vec3 m_pos;
    glm::vec3 m_dir;
    glm::vec3 m_world_up;
    glm::vec3 m_right;
    glm::vec3 m_up;
    float m_canvas_width;
    float m_canvas_height;
    glm::vec3 m_canvas_center_pos;
    glm::vec3 m_canvas_dir_x;
    glm::vec3 m_canvas_dir_y;
    float m_near_plane_dist;
    float m_far_plane_dist;
    int m_screen_width;
    int m_screen_height;
    float m_vertical_fov;
    float m_horizontal_fov;
}
```

Listing 6: Camera class in trac0r. Implementation details are left out for the sake of brevity. The reader should note, however, that many of the attributes shown here are pre-calculated during construction and some are re-calculated every frame.

```
struct Ray {
    glm::vec3 m_origin;
    glm::vec3 m_dir;
    glm::vec3 m_invdir;
};
```

Listing 7: Ray struct in trac0r. `m_invdir` is pre-calculated upon construction.

3.1.5 Random Numbers

Since the Monte Carlo method lives from random sampling, it needs a solid way of generating random numbers. As it turns out, this is actually harder than one might think. While there are a great many algorithms out there for getting random numbers, for the purposes of Monte Carlo integration in a real time path tracing renderer, the

right algorithm has to be chosen very carefully. The most important requirement for this purpose is speed of generation. The C standard library comes with `rand()` but sadly it's unusable for our purposes since it uses global state shared by all threads which makes it effectively single threaded and therefore too slow. The random generators in the C++ standard library provide good quality random numbers but are too slow.

In fact, most random number generators are too slow when having to generate tens of millions of numbers per second. Eventually, it was decided to use `xorshift`-type generators from Sebastiano Vigna [45]. The `xorshift64star` generator is used to provide the seeds for the `xorshift1024star` generator which is in turn used to generate the actual random numbers. Additionally, the `xorshift1024star` generator is very efficient to use on GPUs due to it not using any expensive operations such as divisions, `sqrt` or `pow`.

```
inline uint64_t xorshift64star(uint64_t x) {
    x ^= x >> 12; // a
    x ^= x << 25; // b
    x ^= x >> 27; // c
    return x * 2685821657736338717LL;
}
```

Listing 8: Function to quickly generate random numbers with a short period [45]

```
    inline int64_t xorshift1024star(uint64_t &p, std::array<uint64_t, 16> &s) {
    uint64_t s0 = s[p];
    uint64_t s1 = s[p = (p + 1) & 15];
    s1 ^= s1 << 31; // a
    s1 ^= s1 >> 11; // b
    s0 ^= s0 >> 30; // c
    return (s[p] = s0 ^ s1) * 1181783497276652981LL;
}
```

Listing 9: Function to quickly generate random numbers with a large period [45]

3.1.6 Sampling

trac0r provides a few different methods for geometric sampling.

```
/**
* @brief Selects a random point on a sphere with uniform distribution.
```

```
 * point on a uniform.
 *
 * @return A random point on the surface of a sphere
 */
inline glm::vec3 uniform_sample_sphere() {
    glm::vec3 rand_vec =
    glm::vec3(rand_range(-1.f, 1.f),
    rand_range(-1.f, 1.f),
    rand_range(-1.f, 1.f));
    return glm::normalize(rand_vec);
}
```

Listing 10: Function to sample random points on the surface of a sphere implemented from [46]

```
/**
* @brief Given a direction vector, this will return a random uniform
* point on a sphere on the hemisphere around dir.
*
* @param dir A vector that represents the hemisphere's center
*
* @return A random point the on the hemisphere
*/
inline glm::vec3 oriented_uniform_hemisphere_sample(glm::vec3 dir) {
    glm::vec3 v = uniform_sample_sphere();
    return v * glm::sign(glm::dot(v, dir));
}
```

Listing 11: Function to sample uniform points on a hemisphere given by `dir`

```
/**
* @brief Selects a random point on a sphere with uniform or
* cosine-weighted distribution.
*
* @param dir A vector around which the hemisphere will be centered
* @param power 0.f means uniform distribution while 1.f means
* cosine-weighted
* @param angle When a full hemisphere is desired, use pi/2.
* 0 equals perfect reflection. The value
```

```
 * should therefore be between 0 and pi/2. This angle is equal
 * to half the cone width.
 *
 * @return A random point on the surface of a sphere
 */
inline glm::vec3 sample_hemisphere(glm::vec3 dir, float power, float angle) {
    glm::vec3 o1 = glm::normalize(ortho(dir));
    glm::vec3 o2 = glm::normalize(glm::cross(dir, o1));
    glm::vec2 r = glm::vec2{rand_range(0.f, 1.f),
    rand_range(glm::cos(angle), 1.f)};
    r.x = r.x * glm::two_pi<float>();
    r.y = glm::pow(r.y, 1.f / (power + 1.f));
    float oneminus = glm::sqrt(1.f - r.y * r.y);
    return glm::cos(r.x) * oneminus * o1 +
    glm::sin(r.x) * oneminus * o2 + r.y * dir;
}
```

Listing 12: Function to sample cosine-weighted points on a hemisphere given by `dir`. `power` is used to determine whether to generate uniform samples or cosine-weighted ones. If `power` is `0.f`, uniform samples are generated. If it's `1.f`, cosine-weighted samples are generated. `angle` provides the opening angle of the cone that rays will be generated inside of. [47] [48] [49]

```
/**
* @brief Given a direction vector, this will return a random
* cosine-weighted point on a sphere on the hemisphere around dir.
*
* @param dir A vector that represents the hemisphere's center
*
* @return A random point the on the hemisphere
*/
inline glm::vec3 oriented_cosine_weighted_hemisphere_sample(glm::vec3 dir) {
    return sample_hemisphere(dir, 1.f, glm::half_pi<float>());
}
```

Listing 13: Helper function to get samples from an entire hemisphere making use of the code in listing 12

```
/**
```

```
2  * @brief Selects a random point on a cone with cosine-weighted
3  * distribution.
4  *
5  * @param dir Direction in which the cone is oriented
6  * @param angle Angle of the cone in radians
7  *
8  * @return A random point on the surface of a cone
9  */
10 inline glm::vec3 oriented_cosine_weighted_cone_sample(glm::vec3 dir,
11 float angle) {
12     return sample_hemisphere(dir, 1.f, angle);
13 }
```

Listing 14: Helper function to get samples from a partial hemisphere making use of the code in listing 12

To achieve anti-aliasing, rays are randomly offset within a pixel which results in smoother borders around shapes. This technique is free of additional computational cost with Monte Carlo integration. In comparison, rasterization renderers typically require costly methods such as MSAA, FXAA, MLAA and so on [50] to achieve the same effect.

3.1.7 Russian Roulette

A technique called *Russian roulette* [51] is used for determining when to terminate a ray. This technique is commonly used in Monte Carlo path tracers for this purpose. It works by defining a criterion that is checked against a random value for every ray before the ray is tested for intersection with the scene. If the test is positive, the ray is terminated. Otherwise the ray survives and the probability is multiplied with the ray's energy in order to keep the total energy constant. This technique can be very useful if the criterion is carefully chosen to have a higher chance of terminating rays with lower energy than those with higher energy. The reason for that is that rays with lower energy add little new information to the image as compared to those with high energy.

In this path tracer, the termination criterion used depends on depth as opposed to ray energy because a ray with a higher depth will also typically transfer less energy than one with a low depth. The formula for the termination heuristic in trac0r is

$$\text{continuation\_probability} = 1 - \frac{1}{\text{max\_depth} - \text{depth}}.$$

In code, this is expressed as:

```
float continuation_probability = 1.f - (1.f / (max_depth - depth));
if (rand_range(0.f, 1.0f) >= continuation_probability) {
    break;
}
```

Listing 15: Russian roulette in trac0r

3.1.8 Scene Setup

The scene is hardcoded in the `setup_scene` method of trac0r_viewer. The basic scene setup follows these steps:

1. Set up materials
2. Set up shapes
3. Add shapes to scene
4. Set up camera

The code listed below in 16 creates a basic test scene showing off all of trac0r current materials and shapes. The basic setup resembles that the classic Cornell box. It has a red diffuse left wall, a green diffuse right wall, white floor, white back wall and white ceiling. A glossy box is placed inside the left half of the room while a white diffuse box is placed on the right half of it. A icosahedron with a glass material is placed in its center in front of the boxes. A glossy icosahedron is placed on top of the right box. A box with the emitter material is placed under the ceiling to serve as a light. An almost fully converged picture of this scene can be seen in figure 3.2.

In order to understand the code below refer to the Material listing 2.

```
void Viewer::setup_scene() {
    trac0r::Material emissive{1, {1.f, 0.93f, 0.85f}, 0.f, 1.f, 15.f};
    trac0r::Material default_material{2, {0.740063, 0.742313, 0.733934}};
    trac0r::Material diffuse_red{2, {0.366046, 0.0371827, 0.0416385}};
    trac0r::Material diffuse_green{2, {0.162928, 0.408903, 0.0833759}};
```

```
    trac0r::Material glass{3, {0.5f, 0.5f, 0.9f}, 0.0f, 1.51714f};
    trac0r::Material glossy{4, {1.f, 1.f, 1.f}, 0.09f};

    auto wall_left = trac0r::Shape::make_plane({-0.5f, 0.4f, 0},
                                {0, 0, -glm::half_pi<float>()},
                                {1, 1}, diffuse_red);
    auto wall_right = trac0r::Shape::make_plane({0.5f, 0.4f, 0},
                                {0, 0, glm::half_pi<float>()},
                                {1, 1}, diffuse_green);
    auto wall_back = trac0r::Shape::make_plane({0, 0.4f, 0.5},
                                {-glm::half_pi<float>(), 0, 0},
                                {1, 1}, default_material);
    auto wall_top = trac0r::Shape::make_plane({0, 0.9f, 0},
                                {glm::pi<float>(), 0, 0},
                                {1, 1}, default_material);
    auto wall_bottom = trac0r::Shape::make_plane({0, -0.1f, 0},
                                {0, 0, 0},
                                {1, 1}, default_material);
    auto lamp = trac0r::Shape::make_plane({0, 0.85f, -0.1},
                                {0, 0, 0}, {0.4, 0.4}, emissive);
    auto box1 = trac0r::Shape::make_box({0.3f, 0.1f, 0.1f},
                                {0, 0.6f, 0}, {0.2f, 0.5f, 0.2f},
                                default_material);
    auto box2 = trac0r::Shape::make_box({-0.2f, 0.15f, 0.1f},
                                {0, -0.5f, 0},
                                {0.3f, 0.6f, 0.3f}, glossy);
    auto sphere1 = trac0r::Shape::make_icosphere({0.f, 0.1f, -0.3f},
                                {0, 0, 0}, 0.15f, 2, glass);
    auto sphere2 = trac0r::Shape::make_icosphere({0.3f, 0.45f, 0.1f},
                                {0, 0, 0}, 0.15f, 2, glossy);

    Scene::add_shape(m_scene, wall_left);
    Scene::add_shape(m_scene, wall_right);
    Scene::add_shape(m_scene, wall_back);
    Scene::add_shape(m_scene, wall_top);
    Scene::add_shape(m_scene, wall_bottom);
    Scene::add_shape(m_scene, lamp);
    Scene::add_shape(m_scene, box1);
```

```
44      Scene::add_shape(m_scene, box2);
45      Scene::add_shape(m_scene, sphere1);
46      Scene::add_shape(m_scene, sphere2);
47
48      glm::vec3 cam_pos = {0, 0.31, -1.2};
49      glm::vec3 cam_dir = {0, 0, 1};
50      glm::vec3 world_up = {0, 1, 0};
51
52      m_camera = Camera(cam_pos, cam_dir, world_up, 90.f, 0.001, 100.f,
53      m_screen_width, m_screen_height);
54  }
```

Listing 16: Scene setup in trac0r_viewer

3.1.9 Tracing a Ray

trac0r roughly follows the algorithm outlined in 2.2.2.

```
1  // For every horizontal pixel
2  for (uint32_t x = 0; x < m_width; x += stride_x) {
3      // For every vertical pixel
4      for (uint32_t y = 0; y < m_height; y += stride_y) {
5          // Make a ray out of this pixel
6          Ray ray = Camera::pixel_to_ray(m_camera, x, y);
7
8          // Trace this new ray and save the color
9          glm::vec4 new_color = trace_camera_ray(ray, max_depth);
10
11         // Accumulate result into buffer
12         m_luminance[y * m_width + x] = new_color;
13     }
14 }
```

Listing 17: First, make a ray for every pixel, then trace it, finally accumulate the result into a buffer

```
1  IntersectionInfo intersect(const FlatStructure &flatstruct, const Ray &ray) {
2      IntersectionInfo intersect_info;
3
```

```
4       // Keep track of closest triangle
5       float closest_dist = std::numeric_limits<float>::max();
6       Triangle closest_triangle;
7       for (const auto &shape : FlatStructure::shapes(flatstruct)) {
8           if (intersect_ray_aabb(ray, Shape::aabb(shape))) {
9               for (auto &tri : Shape::triangles(shape)) {
10                  float dist_to_intersect;
11                  bool intersected =
12                      intersect_ray_triangle(ray, tri, dist_to_intersect);
13                  if (intersected) {
14                      // Find closest triangle
15                      if (dist_to_intersect < closest_dist) {
16                          closest_dist = dist_to_intersect;
17                          closest_triangle = tri;
18
19                          intersect_info.m_has_intersected = true;
20                          intersect_info.m_pos =
21                              ray.m_origin + ray.m_dir * closest_dist;
22                          intersect_info.m_incoming_ray = ray;
23
24                          intersect_info.m_angle_between =
25                              glm::dot(closest_triangle.m_normal,
26                                       intersect_info.m_incoming_ray.m_dir);
27
28                          intersect_info.m_normal =
29                              closest_triangle.m_normal;
30                          intersect_info.m_material =
31                              closest_triangle.m_material;
32                      }
33                  }
34              }
35          }
36      }
37
38      return intersect_info;
39  }
```

Listing 18: Scene intersection routine

```
glm::vec4 Renderer::trace_camera_ray(const Ray &ray,
                                     const unsigned max_depth,
                                     const Scene &scene) {
    Ray next_ray = ray;
    glm::vec3 return_color{0.f};
    glm::vec3 luminance{1.f};
    size_t depth = 0;

    // We'll run until terminated by Russian Roulette
    while (true) {
        // Russian Roulette here as defined above
        depth++;

        auto intersect_info = Scene::intersect(scene, next_ray);
        if (intersect_info.m_has_intersected) {
            // Emitter Material
            if (intersect_info.m_material.m_type == 1) {
                return_color =
                    luminance *
                    intersect_info.m_material.m_color *
                    intersect_info.m_material.m_emittance /
                    continuation_probability;
                break;
            }

            // Diffuse Material
            else if (intersect_info.m_material.m_type == 2) {
                // Find normal in correct direction
                intersect_info.m_normal =
                    intersect_info.m_normal *
                    -glm::sign(intersect_info.m_angle_between);
                intersect_info.m_angle_between =
                    intersect_info.m_angle_between *
                    -glm::sign(intersect_info.m_angle_between);

                // Find new random direction for diffuse reflection

                // We're using importance sampling for this since it
```

```
39                  // converges much faster than uniform sampling
40                  glm::vec3 new_ray_dir =
41                      oriented_cosine_weighted_hemisphere_sample(
42                          intersect_info.m_normal);
43                  luminance *= intersect_info.m_material.m_color;
44
45                  // Make a new ray
46                  next_ray = Ray{intersect_info.m_pos, new_ray_dir};
47              }
48
49              // Glass Material
50              else if (intersect_info.m_material.m_type == 3) {
51                  // BRDF Omitted for brevity
52              }
53
54              // Glossy Material
55              else if (intersect_info.m_material.m_type == 4) {
56                  // BRDF Omitted for brevity
57              }
58          } else {
59              break;
60          }
61      }
62
63      return glm::vec4(return_color, 1.f);
64  }
```

Listing 19: Material state machine [49]

3.2 Results

3.2.1 Visual Results

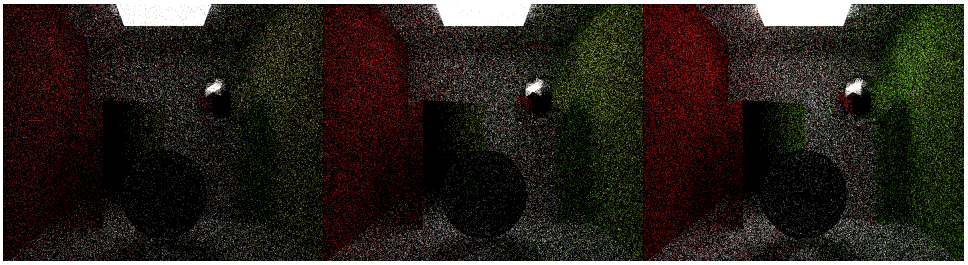

(a) $n = 1$ (b) $n = 2$ (c) $n = 3$

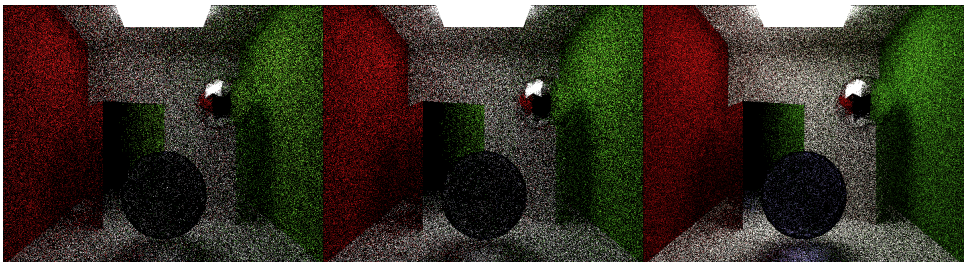

(d) $n = 4$ (e) $n = 5$ (f) $n = 10$

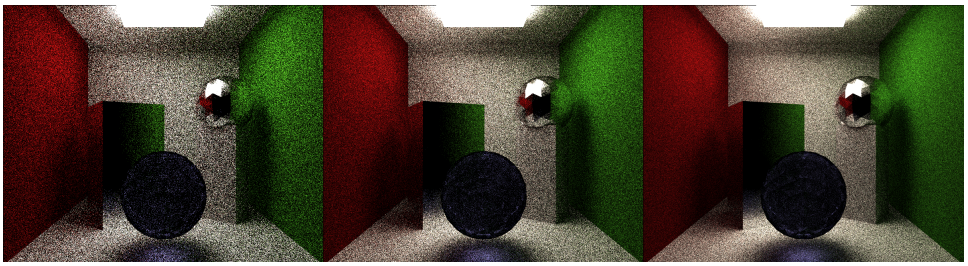

(g) $n = 20$ (h) $n = 50$ (i) $n = 100$

Figure 3.1: trac0r_viewer viewport after integrating n frames

While certainly subjective, frame 3.1h and 3.1i begin to start looking acceptable. It took an average of 10 seconds to approach this kind of acceptable quality at a resolution of 800x640 on an NVIDIA Geforce GTX 570.

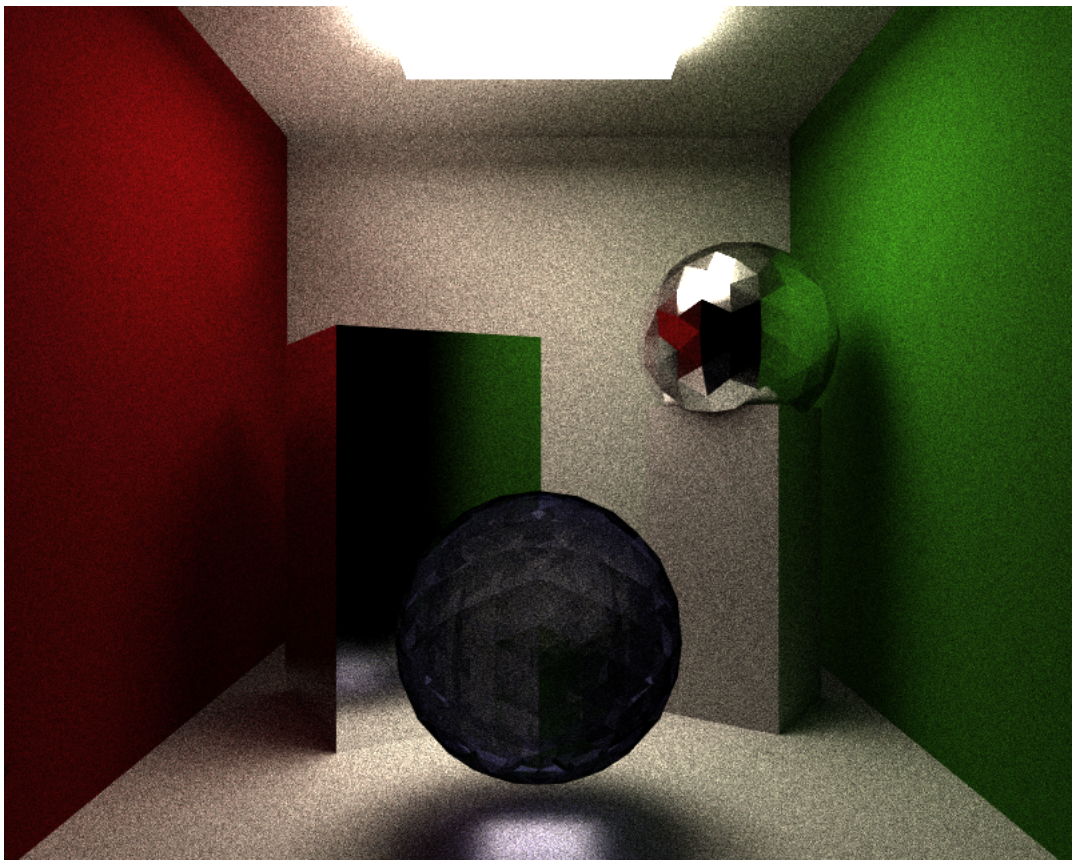

Figure 3.2: trac0r_viewer after integrating for 5000 frames

The image shown in 3.2 displays an almost fully converged image. It took almost 5 minutes to converge to this quality given the same parameters and hardware as above. The scene shown here is described by the code given in listing 16.

3.2.2 Debug View

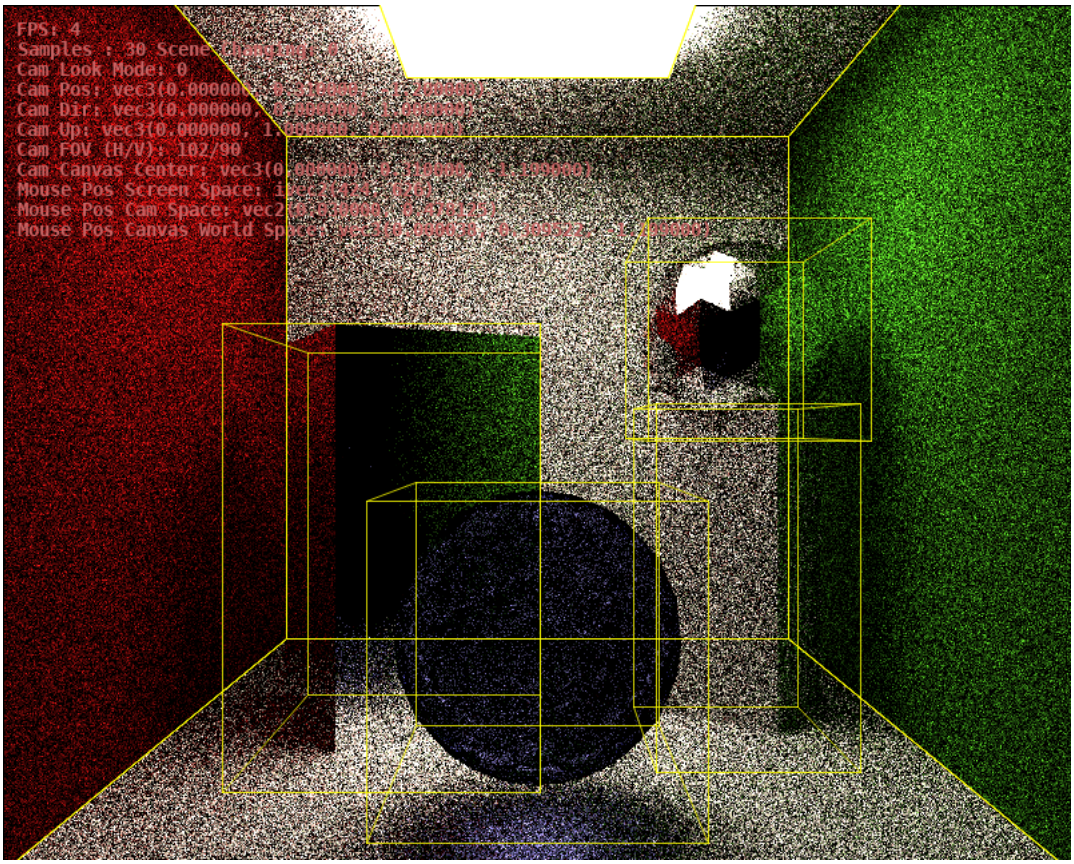

Figure 3.3: trac0r_viewer debug view

Figure 3.3 above shows the debug view that can dynamically toggled during runtime. It displays information about the current state of the camera as well as mouse position and other helpful text in the upper left corner of the viewport. The yellow boxes display the AABBs around the shapes because they are usually not directly visible. This comes in handy when debugging visibility problems.

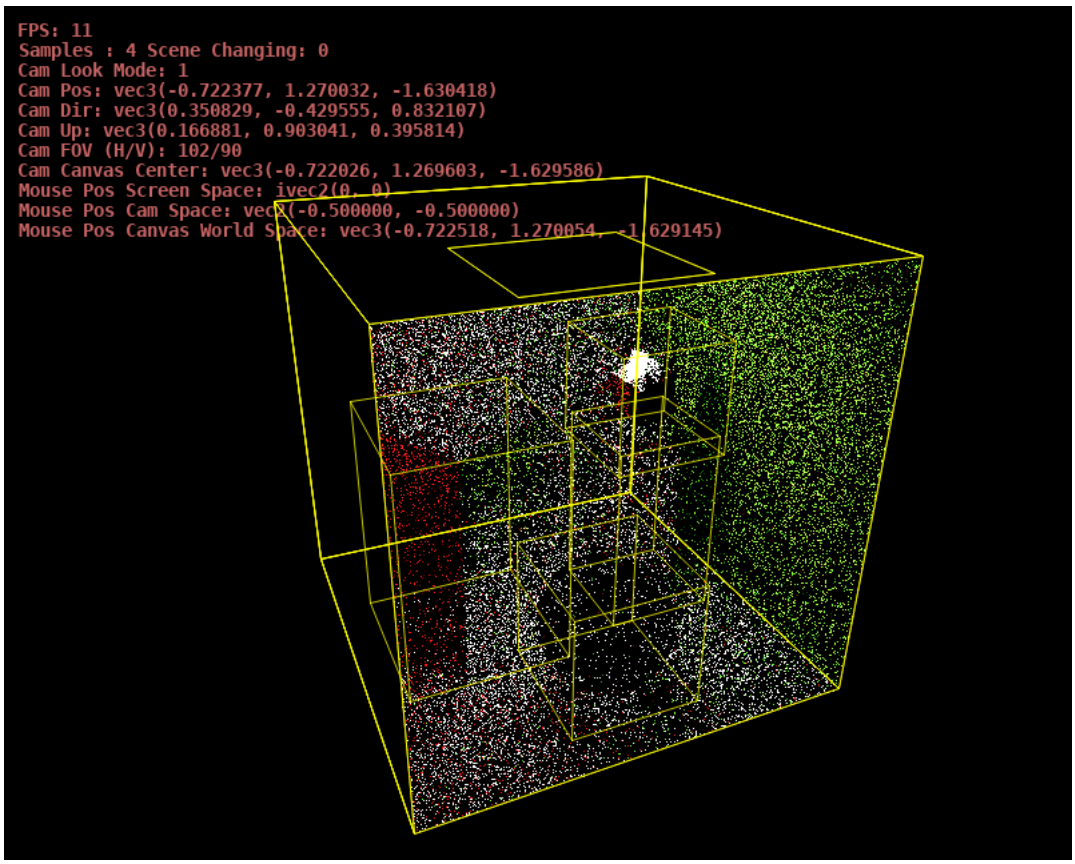

Figure 3.4: trac0r_viewer debug view while interactively navigating the scene

As shown in figure 3.4, trac0r_viewer can be interactively navigated with keyboard and mouse controls to control the camera in the scene. Upon every interaction, the scene rendering begins accumulating samples anew. While the debug view is not necessary for interactivity, it is activated in the image of 3.4 to better show the transformation.

3.2.3 Performance Results

In order to be able to compare performance, an objective and reliable method and unit of measure for doing so has to be decided upon. If this were a rasterizing renderer, FPS would be an easy choice. However, comparing FPS is not a particularly good

criterion between different path tracers since generally FPS doesn't correlate to rate of convergence. That is, one path tracer might be able to iterate at 60 FPS but takes three seconds to converge while a different path tracer may only be able to do 10 FPS but takes only 2 seconds to converge. This might seem unintuitive at first but remember that path tracing is a very different algorithm compared to rasterization. In rasterization, once a frame is rendered, the image is *done*. It won't improve by rendering the same scene a second time. In path tracing, particularly Monte Carlo path tracing, an image will be improved with every new frame that is rendered using the same parameters due to how Monte Carlo integration works.

In spite of that, this thesis uses FPS as the primary criterion for two reasons. Firstly, we are not comparing different path tracers to the one made as part of the thesis. We only compare it against itself in different scene and hardware configurations. Secondly, FPS is much easier to work with and compare than image quality. One might use Peak signal-to-noise ratio (PSNR) to do the latter but that still leaves open the question of when to measure the image as even a single frame might take longer than a second to render under specific circumstances.

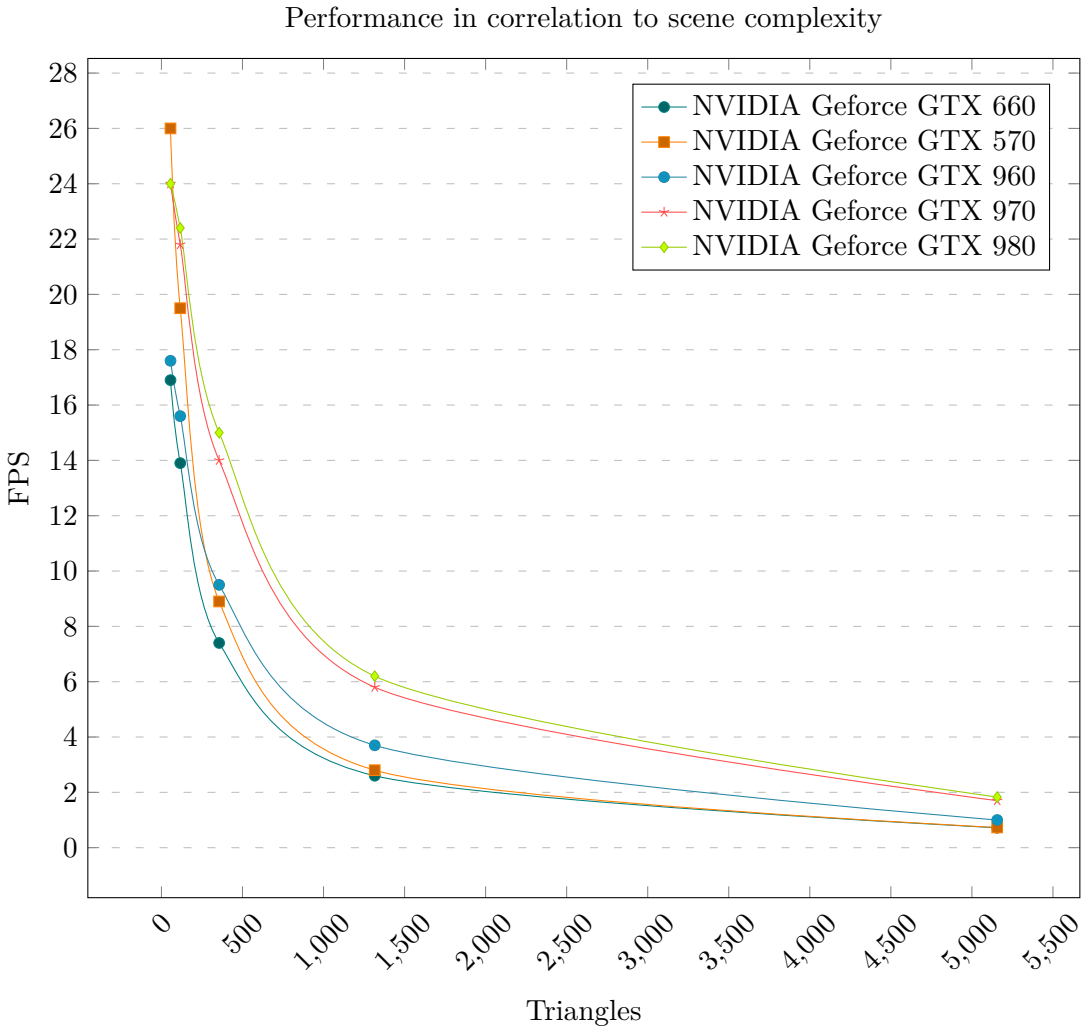

Figure 3.5: Scene complexity benchmark on a variety of graphics cards. It was benchmarked at a resolution of 800x600.

GPU	Average FPS	GFLOPS
NVIDIA Geforce GTX 660	8.3	1881.6
NVIDIA Geforce GTX 570	11.6	1405.4
NVIDIA Geforce GTX 960	9.5	2308
NVIDIA Geforce GTX 970	13.5	3494
NVIDIA Geforce GTX 980	13.9	4612

Table 3.2: Tested GPU performance and GFLOPS

Figure 3.5 shows how FPS behaves in regards to triangle count while table 3.2 shows average FPS per GPU as well as their rated peak single-precision performance in billions of floating point operations per second (GFLOPS).

We can see that the program performs quite poorly as triangle count is increased even at a fairly low number of triangles as predicted with formula 2.1 and in table 2.1.

It is also interesting to see that the difference in performance among the GPUs isn't nearly as dramatic as their rated peak GFLOPS would suggest. This observation suggests that the application is heavily memory bound.

3.3 Evaluation

In order to properly rate the results seen above and in figure 3.5, they need to be put into perspective. Performance of central processing units (CPUs) and GPUs varies enormously depending on their year of release due to technical progress.

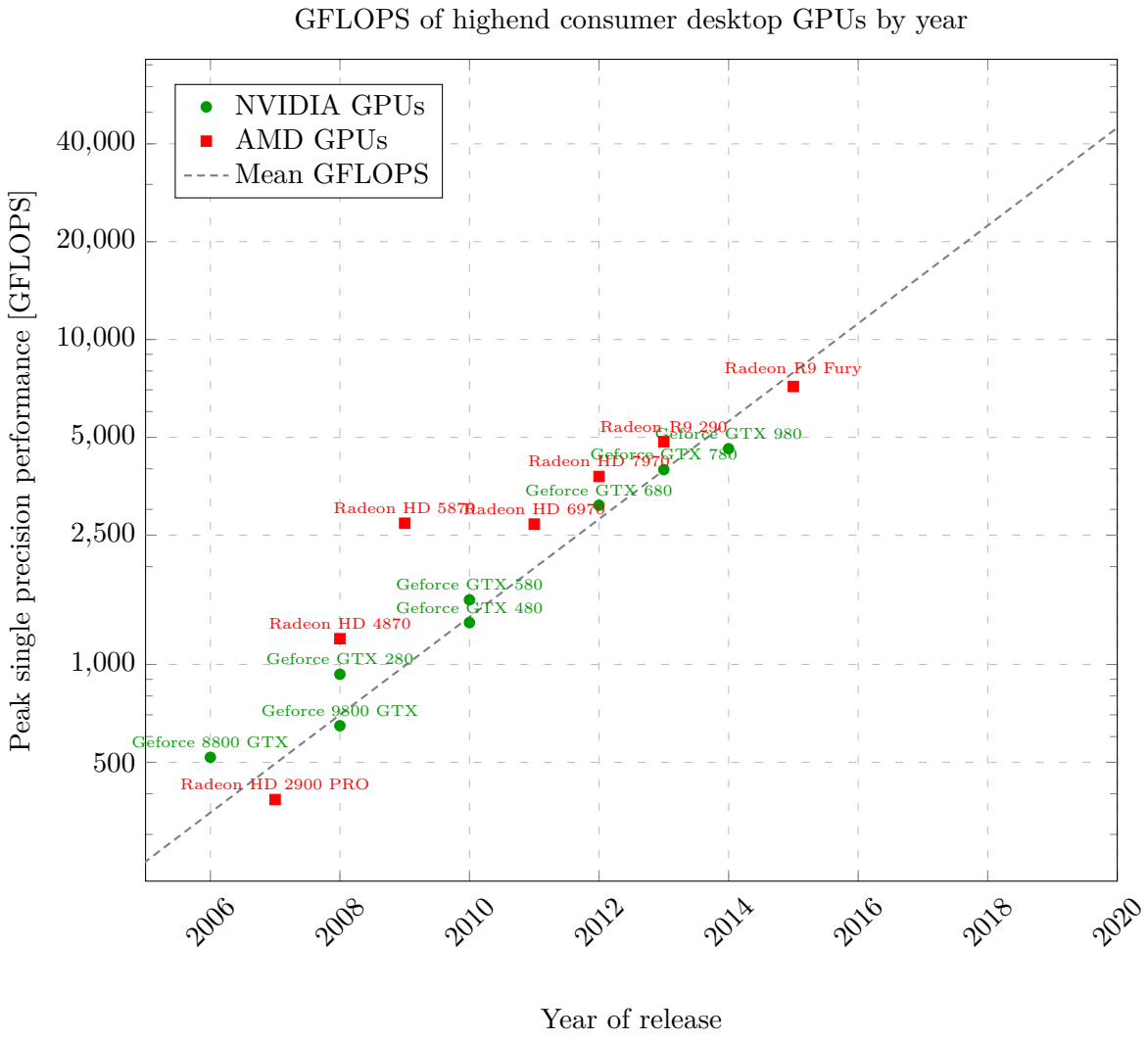

Figure 3.6: Mid-highend GPUs by year vs theoretical single-precision GFLOPS. All GFLOPS numbers are taken from the chip designers' official sites.

The logarithmic graph in figure 3.6 shows the exponential growth of GFLOPS since 2004 when GPUs had approximately 250 GFLOPS of single-precision performance at their disposal. The exponential function of the graph (where x is an integer expressing

the respective year) is

$$f(x) = 250 * 2^{0.5(x-2004)} * 0.7$$

and can be used to extrapolate GPU performance until 2020 assuming the growth stays constant. Following that assumption, there will be a GPU capable of 10000 GFLOPS in 2016, 20000 GFLOPS in 2018 and 40000 GFLOPS in 2020.

It should be noted that while GFLOPS isn't the only relevant criterion to estimating the performance of a GPU, it's likely the most important one.

On the other hand, memory performance didn't keep up with floating point performance and therefore the performance gap between memory and floating point speed widened. This has turned memory latency and memory bandwidth into the most common bottleneck for modern GPU applications.

Although certainly interesting, no graph for memory performance was created because it is much harder to express in a single number since it's usually a multi-tiered memory architecture where each tier has very different sizes and performance characteristics and it also doesn't scale as predictably.

4 Conclusion and Outlook

The study set out to explore the question of when real time path tracing would become a viable alternative to rasterization on consumer-level desktop hardware. It did so by defining performance criteria that were chosen to be considered the minimum threshold for real time path tracing. According to the criteria, real time path tracing would be achieved when a sufficiently converged frame can be rendered within $16.67ms$ (which works out to 60 FPS). The author realizes that image quality is subjective but makes an attempt to be critical about quality.

A Monte Carlo path tracer was implemented as part of the study and is used to benchmark a selection of current and past graphics hardware to extrapolate from. The path tracer was found to be heavily memory bound as the speedup from using a GPU with a better single-precision floating point performance didn't match expectations. Additionally, the path tracer's implementation is mostly naive and therefore doesn't match the current state of the art in terms of algorithmic performance. As such, the benchmark results gained from this path tracer will be used as a lower bound for expected performance.

The study also extrapolates graphics hardware performance by single-precision GFLOPS over the course of 16 years. It was found that GPU performance follows an exponential function and is expected to continue in this manner. Extrapolating the data, single GPUs are expected to reach up to 40 TFLOPS by 2020.

Ongoing research in path tracing and related topics is likely to yield better better algorithms and methods as it has in the past. This is especially true for algorithms specifically meant to run on GPUs as this is still a new topic that has yet to be explored in-depth.

While it is certainly hard to estimate when exactly real time path tracing will be viable, a combination of modern methods for speeding up image convergence is likely to provide satisfactory performance even today on more expensive hardware. The most important improvement over a naive implementation of a path tracer is most certainly found in employing a tree-based acceleration data structure such as a BVH or kd-tree.

This decreases lookup time from $O(n)$ to just $O(\log(n))$ per ray. This would yield an effective speedup of one to two orders of magnitude depending on scene complexity. Convergence performance could best be improved by making use of bidirectional path tracing and better sampling techniques such as *Multiple Importance Sampling*. For scenes that are lit mostly by indirect light, these techniques would lead to faster convergence by about a magnitude.

Apart from algorithmic improvements, the implementation's usage of GPU memory architecture is likely far from optimal and could be improved. GPU memory speeds suggest that this would lead to a general speedup around factor 5.

Lastly, overall image quality could be improved by running an image filter over the rendered image before displaying it to the user. A suitable image filtering algorithm should be non-linear and edge-preserving as well as energy-preserving so that it won't lower the quality of the resulting image. A notable filter fulfilling those requirements is the *bilateral filter*. This could be used to display an image before it is fully converged. This is obviously a trade-off of quality for performance but for the sake of speed it might be worth it.

All in all, the research suggests that real time path tracing could be a viable alternative to rasterization in four years on upper level commodity hardware.

List of Figures

List of Listings

List of Tables

Bibliography

[1] Wikipedia. Caustic (optics) — wikipedia, the free encyclopedia, 2015. [Online; accessed 16-September-2015].

[2] Wikipedia. Dispersion (optics) — wikipedia, the free encyclopedia, 2015. [Online; accessed 16-September-2015].

[3] Wikipedia. Screen space ambient occlusion — wikipedia, the free encyclopedia, 2015. [Online; accessed 16-September-2015].

[4] Wikipedia. Motion blur — wikipedia, the free encyclopedia, 2015. [Online; accessed 16-September-2015].

[5] Wikipedia. Lens flare — wikipedia, the free encyclopedia, 2015. [Online; accessed 16-September-2015].

[6] Wikipedia. Chromatic aberration — wikipedia, the free encyclopedia, 2015. [Online; accessed 16-September-2015].

[7] Wikipedia. Depth of field — wikipedia, the free encyclopedia, 2015. [Online; accessed 16-September-2015].

[8] Wikipedia. Lightmap — wikipedia, the free encyclopedia, 2015. [Online; accessed 16-September-2015].

[9] Eric Veach. *Robust monte carlo methods for light transport simulation.* PhD thesis, Stanford University, 1997.

[10] Eric Lafortune. Mathematical models and monte carlo algorithms for physically based rendering. Technical report, 1996.

[11] Eric Veach and Leonidas J. Guibas. Metropolis light transport. In *Proceedings of the 24th Annual Conference on Computer Graphics and Interactive Techniques*, SIGGRAPH '97, pages 65–76, New York, NY, USA, 1997. ACM Press/Addison-Wesley Publishing Co.

[12] James T. Kajiya. The rendering equation. In *Computer Graphics*, pages 143–150, 1986.

[13] Wikipedia. Volumetric path tracing — wikipedia, the free encyclopedia, 2015. [Online; accessed 11-October-2015].

[14] Eric P Lafortune and Yves D Willems. Rendering participating media with bidirectional path tracing. In *Rendering Techniques' 96*, pages 91–100. Springer, 1996.

[15] Johannes Hanika and Carsten Dachsbacher. Efficient monte carlo rendering with realistic lenses. In *Computer Graphics Forum*, volume 33, pages 323–332. Wiley Online Library, 2014.

[16] Thomas Beneteau. Lambda, 2012. [Online; accessed 11-October-2015].

[17] Ruud van Asseldonk. Luculentus, 2014. [Online; accessed 11-October-2015].

[18] Ruud van Asseldonk. Robigo luculenta, 2015. [Online; accessed 11-October-2015].

[19] Henrik Wann Jensen. Global illumination using photon maps. In *Proceedings of the Eurographics Workshop on Rendering Techniques '96*, pages 21–30, London, UK, UK, 1996. Springer-Verlag.

[20] Cindy M. Goral, Kenneth E. Torrance, Donald P. Greenberg, and Bennett Battaile. Modeling the interaction of light between diffuse surfaces. *SIGGRAPH Comput. Graph.*, 18(3):213–222, January 1984.

[21] Gavin Miller. Efficient algorithms for local and global accessibility shading. In *Proceedings of the 21st Annual Conference on Computer Graphics and Interactive Techniques*, SIGGRAPH '94, pages 319–326, New York, NY, USA, 1994. ACM.

[22] Arthur Appel. Some techniques for shading machine renderings of solids. In *Proceedings of the April 30–May 2, 1968, Spring Joint Computer Conference*, AFIPS '68 (Spring), pages 37–45, New York, NY, USA, 1968. ACM.

[23] Turner Whitted. An improved illumination model for shaded display. *Commun. ACM*, 23(6):343–349, June 1980.

[24] Ernie Wright. The juggler, 1998. [Online; accessed 19-September-2015].

[25] Wikipedia. Toy story — wikipedia, the free encyclopedia, 2015. [Online; accessed 19-September-2015].

[26] Wikipedia. Cars (film) — wikipedia, the free encyclopedia, 2015. [Online; accessed 19-September-2015].

[27] P.H. Christensen, J. Fong, D.M. Laur, and D. Batali. Ray tracing for the movie 'cars'. In *Interactive Ray Tracing 2006, IEEE Symposium on*, pages 1–6, Sept 2006.

[28] Wikipedia. Demoscene — wikipedia, the free encyclopedia, 2015. [Online; accessed 30-September-2015].

[29] Stepan Hrbek. Realtime radiosity, 2015. [Online; accessed 30-September-2015].

[30] Evan Wallace. Webgl path tracing, 2010. [Online; accessed 30-September-2015].

[31] Fairlight. 5 faces, 2013. [Online; accessed 30-September-2015].

[32] Peter da Silva. Raytracing vs rasterization, 2006. [Online; accessed 30-September-2015].

[33] Jeff Atwood. Real-time raytracing, 2008. [Online; accessed 30-September-2015].

[34] John Carmack. Scepticism of real time ray tracing, 2012. [Online; accessed 10-October-2015].

[35] Jacco Bikker and Jeroen van Schijndel. The brigade renderer: A path tracer for real-time games. *Int. J. Computer Games Technology*, 2013:578269:1–578269:14, 2013.

[36] Jacco Bikker and Jeroen van Schijndel. The brigade renderer, 2015. [Online; accessed 09-October-2015].

[37] Jacco Bikker and Jeroen van Schijndel. Octane render, 2015. [Online; accessed 09-October-2015].

[38] Jon Story. Hybrid ray traced shadows, 2015. [Online; accessed 09-October-2015].

[39] David Bucciarelli. Sfera, 2011. [Online; accessed 09-October-2015].

[40] Sven-Hendrik Haase. trac0r, 2015. [Online; accessed 17-January-2016].

[41] Christophe Riccio. Opengl mathematics, 2010. [Online; accessed 09-January-2016].

[42] Wikipedia. Simple directmedia layer — wikipedia, the free encyclopedia, 2016. [Online; accessed 09-January-2016].

[43] Tomas Möller and Ben Trumbore. Fast, minimum storage ray/triangle intersection. In *ACM SIGGRAPH 2005 Courses*, page 7. ACM, 2005.

[44] Wikipedia. Fresnel equations — wikipedia, the free encyclopedia, 2015. [Online; accessed 5-January-2016].

[45] Sebastiano Vigna. xorshift* / xorshift+ generators, 2015. [Online; accessed 11-January-2016].

[46] George Marsaglia et al. Choosing a point from the surface of a sphere. *The Annals*

of Mathematical Statistics, 43(2):645–646, 1972.

[47] Rory Driscoll. Better sampling, 2009. [Online; accessed 14-January-2016].

[48] Unknown. Cosine weighted hemisphere, 2011. [Online; accessed 14-January-2016].

[49] Mikael Hvidtfeldt Christensen. Path tracing 3d fractals, 2015. [Online; accessed 14-January-2016].

[50] Richard Leadbetter. Digital foundry: The future of anti-aliasing, 2011. [Online; accessed 9-January-2016].

[51] Russel E Caflisch. Monte carlo and quasi-monte carlo methods. *Acta numerica*, 7:1–49, 1998.

Eidesstattliche Erklärung

„Hiermit versichere ich an Eides statt, dass ich die vorliegende Arbeit im Studiengang Informatik selbstständig verfasst und keine anderen als die angegebenen Hilfsmittel – insbesondere keine im Quellenverzeichnis nicht benannten Internet-Quellen – benutzt habe. Alle Stellen, die wörtlich oder sinngemäß aus Veröffentlichungen entnommen wurden, sind als solche kenntlich gemacht. Ich versichere weiterhin, dass ich die Arbeit vorher nicht in einem anderen Prüfungsverfahren eingereicht habe und die eingereichte schriftliche Fassung der auf dem elektronischen Speichermedium entspricht."